ChemComm

COMMUNICATION

View Article Online
View Journal

Highly efficient blue-green delayed fluorescence from copper(I) thiolate complexes: luminescence color alteration by orientation change of the aryl ring†

Cite this: DOI: 10.1039/c3cc47871h

Received 14th October 2013,
Accepted 1st December 2013

DOI: 10.1039/c3cc47871h

www.rsc.org/chemcomm

Masahisa Osawa

Highly emissive three-coordinate thiolate copper(I) complexes are synthesized and characterized. The Cu(I) complexes emit intense blue-green delayed fluorescence with high photoluminescence quantum yields of approximately 1.0 at both 293 K and 77 K in the solid state, whereas orange emission at 293 K in solution is observed.

Recently, materials exhibiting thermally activated delayed fluorescence (TADF) with a small singlet–triplet (S–T) energy gap have attracted much attention. This has arisen from their potential importance in the manufacturing of efficient organic light-emitting diodes (OLEDs).[1,2] The most popular phosphors for OLEDs are iridium and other rare metal complexes, which have large S–T gaps and exhibit strong spin–orbit interactions, resulting in highly efficient luminescence performance (almost 100% internal quantum efficiency).[3] In contrast to the rare metal complexes, TADF-type metal complexes have a small S–T gap and weak spin–orbit interaction. Delayed emission mostly occurs from the lowest excited singlet state (S_1) *via* reverse-intersystem crossing from T_1 to S_1 upon thermal activation.[4] When S_1 has a radiative rate constant larger than that for the non-radiative process, TADF-type materials will afford high emission quantum yields.

TADF-type metal complexes with high emission yields are desirable for manufacturing OLEDs because these metals provide a less expensive option than the precious metals that are often required for OLEDs. In this context, we have been investigating luminescent copper(I) complexes. Tetrahedral Cu(I) complexes with low-lying metal-to-ligand charge transfer (MLCT) excited states are known to exhibit TADF, and thus have been extensively studied as luminescent guests for use in OLEDs.[2a–c,5e,f] Copper(I) complexes that exhibit high photoluminescence quantum yields (PLQY) of ≥80% in the solid state are quite common.[5] Actually, three-coordinated Cu(I) complexes with halides emit strong TADF from the transitions (σ + X) → π*.[2d] During the course of this study, we planned to use arylthiolate anions instead of halides aiming at the synthesis of the three coordinated Cu(I) complexes, which afford TADF from the ligand-to-ligand charge transfer (LLCT) transition.

Herein we describe the synthesis and unique photophysical properties of three-coordinate copper(I) complexes, Cu(L_{Me})(SPh) **1** and Cu(L_{iPr})(SPh) **2** L_{Me} = 1,2-bis[bis(2-methylphenyl)phosphino]-benzene, L_{iPr} = 1,2-bis[bis(2-isopropyl)phosphino]benzene.

Complexes **1** and **2** were prepared in 68% and 45% yields, respectively, by mixing Cu(L_{Me})Br for **1** and Cu(L_{iPr})Br for **2** with one equivalent of NaSPh in tetrahydrofuran (THF). Single crystals of **1** and **2** suitable for X-ray analysis were obtained by the solvent layering process, which involved adding diethyl ether on the surface of saturated solutions of the complexes in THF.

Single crystal X-ray diffraction studies of **1** and **2** revealed monomeric three-coordinate structures. The molecular structure of **1** is shown in Fig. 1 as an example. The coordination geometries of the copper centers in **1** and **2** are trigonal planar; the sum of the angles around the Cu(I) center is 359.63° for **1** and 359.59° for **2**. The distances of the Cu–P bonds (2.2409–2.2633 Å for **1** and **2**) are almost equal to those in Cu(L_{Me})Br.[2d] Another notable feature is that the aryl ring including the –SPh moiety is

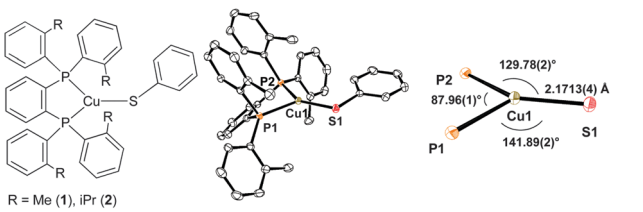

Fig. 1 Left: molecular structures of **1** and **2**. Center: ORTEP view of **1**. Thermal ellipsoids are drawn at the 50% probability level. Hydrogen atoms are omitted for clarity. Right: core structure of **1**.

Molecular Spectroscopy Laboratory, RIKEN, Hirosawa 2-1, Wako-Shi, 351-0198, Japan. E-mail: osawa@postman.riken.jp

† Electronic supplementary information (ESI) available: Synthetic details, characterization data, and temperature dependence of decay time for **1** and **2**. CCDC 960819 for **1** and 960820 for **2**. For ESI and crystallographic data in CIF or other electronic format see DOI: 10.1039/c3cc47871h

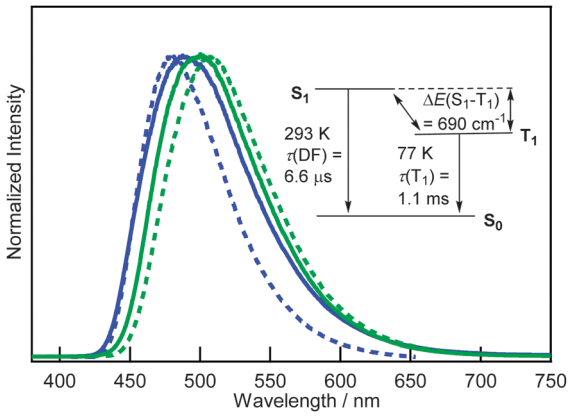

Fig. 2 Emission spectra of **1** (blue line) and **2** (green line) in the solid state at 293 K (solid) and 77 K (dashed). The inset displays the energy gap between S_1 and T_1 levels of **1**.

coplanar with the metal plane consisting of Cu(I), S, and two P atoms in **1** and **2**: the dihedral angle between the metal plane and the aryl ring is as small as 4.72(6)° for **1** and 2.75(5)° for **2**.

Emission spectra of **1** and **2** at 293 K and 77 K in the solid state are presented in Fig. 2. Table 1 provides a summary of the emission maxima (λ_{max}), lifetimes (τ), and photoluminescence quantum yields (Φ_{PL}) of **1**, **2**, and Cu(L_{Me})Br at 293 and 77 K, as well as the energy gaps between S_1 and T_1 ($\Delta E(S_1–T_1)$). Complexes **1** and **2** exhibit efficient blue-green emission with peak maxima at 488 nm for **1** and 500 nm for **2**, and PLQYs of ~1.0 for both **1** and **2** at 293 K. PLQYs in the solid state at 293 K are found to increase by *ca.* two times by substituting the bromide for the benzothiolate anion (Table 1). Emission bands are broad, and their lifetimes are as short as 6.6 μs for **1** and 5.0 μs for **2** at 293 K. It is noted that, although the lifetimes are markedly different for **1** at 293 K and 77 K, the emission peak wavelength of **1** at 293 K is very close to that at 77 K. Molecular orbital (MO) calculations revealed that the major transitions (~95%) that contribute to emission from **1** and **2** ($T_1 \rightarrow S_0$ and $S_1 \rightarrow S_0$) were attributed to two types of ligand-to-ligand charge-transfer (LLCT) processes. One is the charge transfer from the sulfur atom to an empty antibonding π orbital on the phenylene and tolyl rings in the diphosphine ligand ($S \rightarrow \pi^*$), and the other is from a π orbital on the aryl ring of the thiolate ligand to an empty antibonding π orbital on the phenylene and tolyl rings in the diphosphine ligand ($\pi \rightarrow \pi^*$) (see Tables S3–S6 and Fig. S3–S6 in the ESI†). Conversely, MLCT contributions are very small (~2–3% for **1** and **2**).

Table 1 Photophysical properties of **1**, **2**, and Cu(L_{Me})Br in the solid state

	λ_{max}[a]/nm (τ[b]/μs)		Φ_{PL}[c]		
	T = 293 K	T = 77 K	T = 293 K	T = 77 K	$\Delta E(S_1–T_1)$[d]/cm^{-1}
1	488 (6.6)	481 (1100)	0.95	0.95	690
2	500 (5.0)	504 (1900)	0.95	0.95	630
Cu(L_{Me})Br[e]	512 (8.0)	500 (360)	0.55	0.85	—

[a] Emission maximum; λ_{exc} = 355 nm. [b] Emission decay time; λ_{exc} = 355 nm. [c] Absolute PL quantum yield in the solid state (error ± 5%). [d] Energy gap between S_1 and T_1 levels obtained by temperature dependence of decay time (see Fig. S8 and S9 in the ESI). [e] For comparison.[2d]

Small S_1–T_1 gaps ($\Delta E(S_1–T_1) < 700$ cm^{-1}; see Fig. S8 and S9 in the ESI†), obtained by fitting the temperature dependence of decay times in Table 1, strongly indicate that emission from **1** and **2** in the solid state at room temperature can be ascribed to TADF, which occurs when the S_1–T_1 gap is small enough to achieve a thermal equilibrium between the two states (the inset in Fig. 1). According to the TADF theory,[4d] cooling the luminescent sample results in the red-shift of the emission peak. Complex **1**, however, exhibits a slight blue shift on going from 293 to 77 K. Presumably, the ground state of **1** in crystals is stabilized in energy at low temperatures by molecular interactions.

Fig. 3 shows the absorption spectra of ligand L_{Me} and complex **1** as well as the corrected emission spectra of **1** in 2-methyltetrahydrofuran (2-MeTHF) at 298 K and 77 K. Both L_{Me} and **1** exhibit absorption peaks with a similar molar absorption coefficient ($\varepsilon \approx 20\,000$ M^{-1} cm^{-1}) around 290 nm. However, complex **1** shows an additional broad shoulder at approximately 330 nm. Photoluminescence properties of **1**, **2**, Cu(L_{Me})Br, and Cu(L_{iPr})Br in 2-MeTHF are summarized in Table 2. **1** gives bright blue emission with λ_{max} = 466 nm, τ = 1.3 ms and Φ_{PL} = 1.0 in 2-MeTHF at 77 K, and orange emission with λ_{max} = 592 nm, τ = 1.4 μs and Φ_{PL} = 0.24 at 293 K. Since, upon increasing the temperature from 77 to 293 K, (1) the emission peak of **1** is red-shifted by 130 nm, (2) PLQY decreases from 1.0 to 0.24, and (3) emission lifetime becomes three orders of magnitude shorter, we assume that **1** undergoes a structural change in the emissive excited state. The radiative rate constants k_r and the non-radiative rate constants k_{nr} are listed in Table S3 in ESI.† The blue phosphorescence observed for **1** in 2-MeTHF at 77 K is explained by assuming that structural changes in a low-temperature frozen medium are minimal in the excited states, and thus emission occurs from the T_1 state with the ground state structure, which is determined by X-ray diffraction studies in the solid state. In fact, the phosphorescence spectrum and the lifetime observed in frozen 2-MeTHF are very close to those observed in the solid state at 77 K.

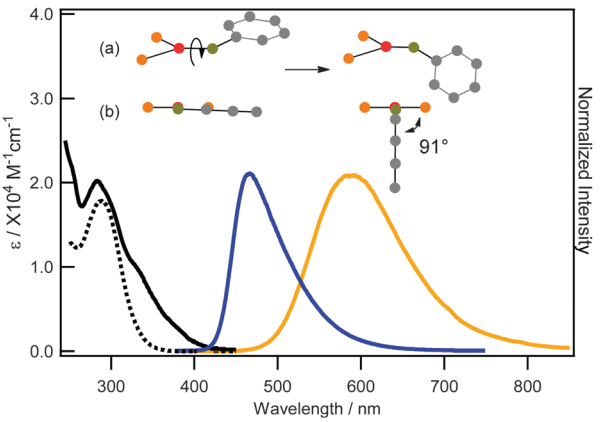

Fig. 3 Absorption spectra of L_{Me} (black dashed line) and **1** (black solid line) in 2-MeTHF and emission spectra of **1** in 2-MeTHF at 293 K (orange line) and at 77 K (blue line). The inset shows (a) the structural change of **1** in the excited state; (b) the side view.

Table 2 Photophysical properties of **1**, **2**, Cu(L_{Me})Br, and Cu(L_{iPr})Br in 2-MeTHF

	λ_{max}[a]/nm (τ[b]/μs)		Φ_{PL}[c]	
	T = 293 K	T = 77 K	T = 293 K	T = 77 K
1	592 (1.4)	466 (1300)	0.24	0.95
2	546 (1.0)	492 (2300)	0.15	0.95
Cu(L_{Me})Br[d]	523 (4.2)	506 (1900)	0.40	0.93
Cu(L_{iPr})Br[d]	519 (7.7)	501 (1000)	0.50	0.90

[a] Emission maximum; λ_{exc} = 355 nm. [b] Emission decay time; λ_{exc} = 355 nm. [c] Absolute PL quantum yield in solution (error ± 5%). [d] For comparison.

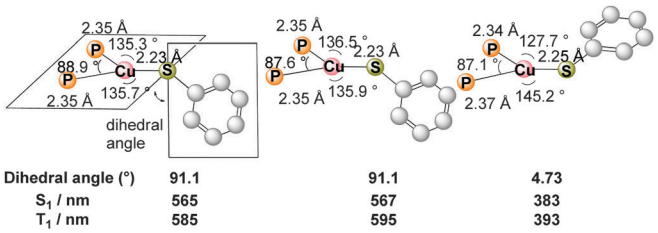

Fig. 4 Optimized core structures of **1** in the singlet (left) and the triplet (center) excited state and the ground state (right); dihedral angles, and S_1 and T_1 energies of each optimized structure.

MO calculations indicate that the structural change was based on the rotation of the –SPh-containing aryl ring about the axis of the Cu–S bond (see the inset in Fig. 3). As represented in Fig. 4, the calculations provide confirmation of the lowering of energies of the S_1 and T_1 states, which are responsible for the red-shift of the emission peaks; the metal plane and the aryl ring, which are coplanar in the ground state (S_0), are perpendicular to each other in S_1 and T_1 states (dihedral angles between the metal plane and aryl ring are 91.1°). However, the trigonal planar core structure, which consists of Cu(I), sulfur, and two phosphorous atoms, remains unchanged even in the excited states, suggesting that this structural change is different from a Jahn–Teller type distortion observed in trigonal planar Au(I) complexes.[6] Small S_1–T_1 energy gaps (605 cm^{-1} and 830 cm^{-1}, see Fig. 4) in both the optimized structures suggest that the orange emission observed is due to TADF. The S_1 energy obtained by MO calculations for **1** is in good accord with the peak energy at 293 K (Fig. 4 and Table 2). In comparison with **1**, **2** does not exhibit a large red-shift (54 nm, as seen in Table 2) probably because the aryl ring cannot turn to the orthogonal position owing to the bulky iPr groups on the metal side (see Fig. S7 in the ESI†). Furthermore, we found that three-coordinated copper(I) complexes Cu(L_{Me})Br and Cu(L_{iPr})Br do not show large red-shift of emission by warming from 77 K to 293 K (Table 2). This result strongly supports the assumption that luminescence color alteration is due to orientation change of the thiolate aryl ring.

In conclusion, highly emissive three-coordinate thiolate copper(I) complexes were obtained in good yields. The change in orientation of the –SPh-containing aryl ring is found to dramatically alter the optical properties of **1** and **2** in solution. Application of **1** and **2** in TADF-type OLEDs is now in progress.

This work was supported by the Japan Society of the Promotion of Science (Grant-in-Aid for Scientific Research; No. 25410080). We acknowledge Dr Daisuke Hashizume for technical assistance with X-ray structural analysis.

Notes and references

1 (*a*) H. Uoyama, K. Goushi, K. Shizu, H. Nomura and C. Adachi, *Nature*, 2012, **492**, 234–238; (*b*) Q. Zhang, J. Li, K. Shizu, S. Huang, S. Hirata, H. Miyazaki and C. Adachi, *J. Am. Chem. Soc.*, 2012, **134**, 14706–14709; (*c*) F. B. Dias, K. N. Bourdakos, V. Jankus, K. C. Moss, K. T. Kamtekar, V. Bhalla, J. Santos, M. R. Bryce and A. P. Monkman, *Adv. Mater.*, 2013, **25**, 3707–3714.

2 (*a*) M. Osawa, I. Kawata, R. Ishii, S. Igawa, M. Hashimoto and M. Hoshino, *J. Mater. Chem. C*, 2013, **1**, 4375–4383; (*b*) S. Igawa, M. Hashimoto, I. Kawata, M. Yashima, M. Hoshino and M. Osawa, *J. Mater. Chem. C*, 2013, **1**, 542–551; (*c*) J. C. Deaton, S. C. Switalski, D. Y. Kondakov, R. H. Young, T. D. Pawlik, D. J. Giesen, S. B. Harkins, A. J. M. Miller, S. F. Mickenberg and J. C. Peters, *J. Am. Chem. Soc.*, 2010, **132**, 9499–9508; (*d*) M. Hashimoto, S. Igawa, M. Yashima, I. Kawata, M. Hoshino and M. Osawa, *J. Am. Chem. Soc.*, 2011, **133**, 10348–10351.

3 (*a*) M. A. Baldo, S. Lamansky, P. E. Burrows, M. E. Thompson and S. R. Forrest, *Appl. Phys. Lett.*, 1999, **75**, 4–6; (*b*) M. A. Baldo, M. E. Thompson and S. R. Forrest, *Nature*, 2000, **403**, 750–753; (*c*) C. Adachi, M. A. Baldo, M. E. Thompson and S. R. Forrest, *J. Appl. Phys.*, 2001, **90**, 5048–5051; (*d*) D. Tanaka, H. Sasabe, Y.-J. Li, S.-J. Su, T. Takeda and J. Kido, *Jpn. J. Appl. Phys., Part 2*, 2007, **46**, L10–L12; (*e*) D. Tanaka, Y. Agata, T. Takeda, S. Watanabe and J. Kido, *Jpn. J. Appl. Phys., Part 2*, 2007, **46**, L117C–L119C.

4 (*a*) C. A. Parker, in *Advanced in Photochemistry*, ed. W. A. Noyes, Jr., G. S. Hammond and J. N. Pitts, Jr., John Wiley & Sons, Inc., New York, 1964, vol. 2, pp. 305–383; (*b*) G. Blasse and D. R. McMillin, *Chem. Phys. Lett.*, 1980, **70**, 1–3; (*c*) D. Felder, J.-F. Nierengarten, F. Barigelletti, B. Ventura and N. Armaroli, *J. Am. Chem. Soc.*, 2001, **123**, 6291–6299; (*d*) H. Yersin, A. F. Rausch, R. Czerwieniec, T. Hofbeck and T. Fischer, *Coord. Chem. Rev.*, 2011, **255**, 2622–2652; (*e*) H. Yersin, A. F. Rausch and R. Czerwieniec, in *Phys. Org. Semicond.*, ed. W. Bruettig, C. Adachi and R. J. Holmes, Wiley-VCH, Weinheim, 2nd edn, 2012, pp. 371–424.

5 (*a*) R. Czerwieniec, J.-B. Yu and H. Yersin, *Inorg. Chem.*, 2011, **50**, 8293–8301; (*b*) R. Czerwieniec, K. Kowalski and H. Yersin, *Dalton Trans.*, 2013, **42**, 9826–9830; (*c*) J.-L. Chen, X.-F. Cao, J.-Y. Wang, L.-H. He, Z.-Y. Liu, H.-R. Wen and Z.-N. Chen, *Inorg. Chem.*, 2013, **52**, 9727–9740; (*d*) L. Bergmann, J. Friedrichs, M. Mydlak, T. Baumann, M. Nieger and S. Braese, *Chem. Commun.*, 2013, **49**, 6501–6503; (*e*) D. M. Zink, M. Baechle, T. Baumann, M. Nieger, M. Kuehn, C. Wang, W. Klopper, U. Monkowius, T. Hofbeck, H. Yersin and S. Braese, *Inorg. Chem.*, 2013, **52**, 2292–2305; (*f*) D. Volz, D. M. Zink, T. Bocksrocker, J. Friedrichs, M. Nieger, T. Baumann, U. Lemmer and S. Braese, *Chem. Mater.*, 2013, **25**, 3414–3426; (*g*) X.-L. Chen, R. Yu, Q.-K. Zhang, L.-J. Zhou, X.-Y. Wu, Q. Zhang and C.-Z. Lu, *Chem. Mater.*, 2013, **25**, 3910–3920.

6 K. A. Barakat, T. R. Cundari and M. A. Omary, *J. Am. Chem. Soc.*, 2003, **125**, 14228–14229.